ISSN (Print) : 2320 – 3765
ISSN (Online): 2278 – 8875

International Journal of Advanced Research in Electrical, Electronics and Instrumentation Engineering

(A High Impact Factor, Monthly, Peer Reviewed Journal)

Website: www.ijareeie.com

Vol. 7, Issue 11, November 2018

Artificial Neural Network for Control and Grid Integration of Floating Solar Photovoltaic System

S.Sathiya Bama, Dr. K.Punitha

PG Scholar, Department of Electrical and Electrical Engineering, P.S.R.Rengasamy College of Engineering for Women, Sivakasi, Tamilnadu, India

Head of the Department, Department of Electrical and Electrical Engineering, P.S.R.Rengasamy College of Engineering for Women, Sivakasi, Tamilnadu, India

ABSTRACT: Solar photovoltaic (PV) energy is becoming an increasingly important part of the world's renewable energy. Even though solar power generation has several advantages over other forms of electricity generation, the major problem is the requirement of land which is scarcely available in the world and its cost. In this project refers to riverbed solar panel, these solar panels that float on a body of water. This technique would prove to be a revolutionary step as it could solve the perennial problem of land. A rivertop solar PV system should maximize the power output from the PV array while ensuring overall system performance, safety, reliability, and controllability for interface with the electricity grid. This paper main objective is: To develop an incremental conductance based MPPT for DC-DC converter; To develop an approximate dynamic programming (ADP) based artificial neural network (ANN) vector control strategy for a LCL-filter based single phase solar inverter. To evaluate the performance of the rivertop solar PV system under varies environmental condition. The result demonstrate river top PV system using the conventional standard vector control method and proportional resonant control method in MATLAB simulation. This is also true in the presence of noise, disturbance, distortion, and non-ideal conditions.

I. INTRODUCTION

The global market for grid-connected residential solar photovoltaic (PV) installations is anticipated to keep growing to reach more than 900 MW in 2018. A grid connected residential solar PV system normally consists two parts: 1) a PV array that generates electricity from solar irradiance and 2) power electronic converters for energy extraction and grid integration. A PV array is built by certain series and parallel connection of many solar cells together. There are two major issues concerning a solar PV system: maximum power extraction from a PV array and efficient and stable grid integration.

The power generated from a PV array generally relies on the temperature and solar irradiance level. For each solar irradiance and temperature condition, a unique point, called maximum power point (MPP), can be found from the P-V curve, at which the PV array produces its maximum possible output power. The location of the MPP can be located by applying a maximum power point tracking (MPPT) algorithm, which can be achieved by controlling the DC-DC converter connected to the PV array. The primary requirements for control of a solar PV system by using an MPPT algorithm include the abilities to: 1) locate an MPP quickly and accurately, 2) maintain the same MPP of a PV system when weather condition remains unchanged, and 3) track a correct MPP under fast changing irradiance conditions.

To integrate a rivertop solar PV systems into the grid, a single-phase DC-AC inverter is commonly introduced and a control strategy for the single-phase inverter needs to be applied to guarantee the stability of the whole system. The inverter must maintain a stable DC-link voltage in order to assure efficient and reliable MPPT operation, which is a challenging task especially under fast changing weather conditions.

The purpose of this paper is to investigate how to realize ADP-ANN vector control technology for a residential solar PV system, how the ADP-ANN technology benefits the energy extraction from a PV array and the integration of the

PV array to the grid, and how the ADP-ANN technology is compared with conventional methods for grid integration and control of residential PV systems. The primary contributions of the paper include an ADP-ANN based control method for LCL-filter based single-phase PV systems and combination of MPPT and ADP-ANN control techniques for solar energy extraction and grid integration. The paper investigates the ADP-ANN based residential PV system in terms of energy capture efficiency, DC-link voltage stability, adaptively, power conversion efficiency, power quality, etc.

II. RELAED WORK

Blaabjerg et al.[1] Digital implementation of this derivative term is generally a challenge with many methods presently developed for resolving it. These methods are however still facing drawbacks, which have comprehensively been explained in the paper. Two derivatives are then proposed, based on either second-order or non-ideal generalized integrator.

Lin et al [2], proposed RFCMANN controller uses the signed distance and input space repartition mechanisms to convert the dual input variables to sole input variable and repartition the input space to an appropriate quantity. Therefore, the structure and computation complexities of the proposed RFCMANN controller are effectively reduced and make it more practical.

Yang et al. [3], proposed intelligent controller regulates the value of reactive power to a new reference value which complies with the regulations of LVRT under grid faults. Moreover, a dual mode operation control method of the converter and inverter of the three-phase grid-connected PV system is designed to eliminate the fluctuation of DC-link bus voltage under grid faults.

X. Fu and S. Li et al. [4], proposes a novel recurrent neural network based vector control method for a single-phase inverter with an LCL filter. The neural network is trained based on adaptive dynamic programming principle and the objective of the training is to approximate optimal control. The Levenberg-Marquardt plus Forward Accumulation through Time algorithm is developed for training the proposed recurrent neural network controller. The neural network vector control approach is compared with conventional control methods, including the conventional PI-based vector control method and the PR-based control technique for single-phase inverters.

Wang et al. [5], presents an effective control scheme using a line-commutated high-voltage direct-current (LCC-HVDC) link joined with a damping controller based on adaptive-network-based fuzzy inference system (ANFIS) to achieve damping improvement of an integration of wind, solar, and marine-current power systems fed to a synchronous generator (SG)-based power system. The proposed ANFIS is an adaptive, robustness controller by combining the advantages of artificial neural network and fuzzy logic controller to face different operating conditions of the studied system. A time-domain scheme based on a nonlinear-system model subject to a three-phase short-circuit fault at the infinite bus is utilized to examine the effectiveness of the proposed control schemes.

III. SYSTEM IMPLEMENTATION

A) EXISTING SYSTEM

Existing technologies, vector control is usually used to control a three-phase solar inverter. However, to applying vector control to a single-phase inverter, an imaginary circuit needs to be created, which has caused challenges to ensure high performance of vector control in residential solar PV applications, including low reliability under variable PV power generation condition and high harmonic distortion. At present, the dominate control strategies for a single-phase inverter are proportional resonant (PR) control and sliding mode control (SMC) based upon hysteresis switching mechanisms. Compared to vector control, both require a high sampling frequency (e.g., 10s or 100s kHz) and switching frequency (e.g., 10s or 100s kHz), which would cause more energy loss, larger size of heat sink, and more expensive inverter systems.

B) PROPOSED SYSTEM

The proposed system, to investigate an artificial neural network (ANN) control strategy based on approximate dynamic programming (ADP) for optimal control and grid integration of residential solar PV systems. The purpose of this project is to investigate how to realize ADP-ANN vector control technology for a residential solar PV system, how the ADP-ANN technology benefits the energy extraction from a PV array and the integration of the PV array to the grid, and how the ADP-ANN technology is compared with conventional methods for grid integration and control of residential PV systems. The primary contributions of the paper include an ADP-ANN based control method for LCL-filter based single-phase PV systems and combination of MPPT and ADP-ANN control techniques for solar energy extraction and grid integration. The paper investigates the ADP-ANN based residential PV system in terms of energy capture efficiency, DC-link voltage stability, adaptivity, power conversion efficiency, power quality, etc.

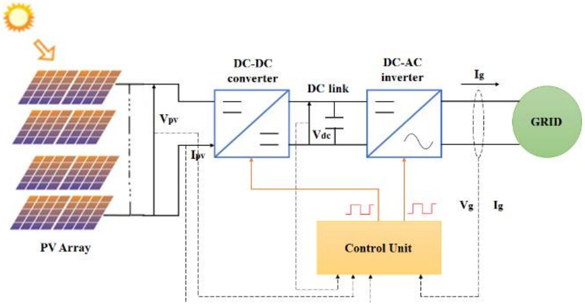

Figure 1 Proposed block

i)Description:

A residential solar PV system usually includes five parts, an array of PV panels, a DC-DC converter for energy capture from the PV array, a single-phase inverter for grid integration, a DC-link capacitor between the inverter and DC-DC converter, and an integrated control unit. PV panels are connected to form an array to produce desired level of voltage and current. In order to get maximum output power from a PV system, the MPP of the system needs to be continuously tracked, which can be achieved by controlling the DC-DC converter that connects the PV array to the DC-link capacitor. Incremental Conductance (IC) method is one of the most popular and widely used, it is theoretically possible to locate the operating point at a MPP when the perturbation stops. Artificial neural networks for MPPT control method used. The solar inverter converts the DC output from the DC-DC converter to AC in order for the PV array to be integrated into the grid.

ii) Conventional Vector Control

To implement *d-q* vector control for a single-phase inverter, an imaginary orthogonal circuit of the real circuit is needed. The imaginary circuit has the same circuit components as those shown in the real circuit; the AC voltage and current in the imaginary circuit have the same amplitudes as those of the real circuit but with -90^o phase shift. Fig. 4 shows both the real and imaginary circuits. The corresponding variables of the imaginary circuit are marked with '*im*'. The real and imaginary circuits make up the *α-β* frame of the single-phase system, which is then transferred into the *d-q* frame through (1). The relations between variables in *α-β* and *d-q* domains are:

are: $v_g, v^{im}_g \leftrightarrow v_{g\_d}, v_{g\_q}$; $i_g, i^{im}_g \leftrightarrow i_{g\_d}, i_{g\_q}$; $i_{inv}, i^{im}_{inv} \leftrightarrow i_{inv\_d}, i_{inv\_q}$; $v_c, v^{im}_c \leftrightarrow v_{c\_d}, v_{c\_q}$; $v_{inv}, v^{im}_{inv} \leftrightarrow v_{inv\_d}, v_{inv\_q}$.

$$T_{\alpha\beta\_dq} = \begin{bmatrix} \cos(\omega t) & \sin(\omega t) \\ -\sin(\omega t) & \cos(\omega t) \end{bmatrix} \quad \text{----- (1)}$$

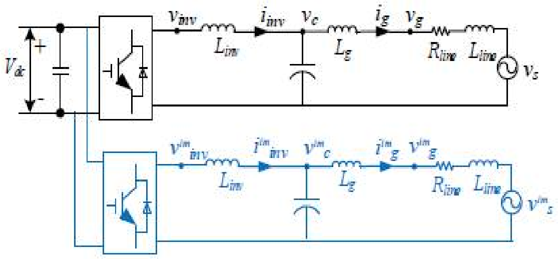

Fig. 4. LCL-filter PV inverter schematic: real and imaginary circuits

ISSN (Print) : 2320 – 3765
ISSN (Online): 2278 – 8875

International Journal of Advanced Research in Electrical, Electronics and Instrumentation Engineering

(A High Impact Factor, Monthly, Peer Reviewed Journal)

Website: www.ijareeie.com

Vol. 7, Issue 11, November 2018

Three equations in *d-q* frame can be obtained from Fig. 4. They are: voltage balance equation across the grid-side inductor *Lg* (2); voltage balance equation across the inverter side inductor *Linv* (3); current balance equation across the *LCL*
capacitor *C* (4):

$$\begin{bmatrix} v_{c\_d} \\ v_{c\_q} \end{bmatrix} = R_g \begin{bmatrix} i_{g\_d} \\ i_{g\_q} \end{bmatrix} + L_g \frac{d}{dt} \begin{bmatrix} i_{g\_d} \\ i_{g\_q} \end{bmatrix} + \omega L_g \begin{bmatrix} -i_{g\_q} \\ i_{g\_d} \end{bmatrix} + \begin{bmatrix} v_{g\_d} \\ v_{g\_q} \end{bmatrix} \quad - 2$$

$$\begin{bmatrix} v_{inv\_d} \\ v_{inv\_q} \end{bmatrix} = R_{inv} \begin{bmatrix} i_{inv\_d} \\ i_{inv\_q} \end{bmatrix} + L_{inv} \frac{d}{dt} \begin{bmatrix} i_{inv\_d} \\ i_{inv\_q} \end{bmatrix} + \omega L_{inv} \begin{bmatrix} -i_{inv\_q} \\ i_{inv\_d} \end{bmatrix} + \begin{bmatrix} v_{c\_d} \\ v_{c\_q} \end{bmatrix} \quad -3$$

$$\begin{bmatrix} i_{inv\_d} \\ i_{inv\_q} \end{bmatrix} = \begin{bmatrix} i_{g\_d} \\ i_{g\_q} \end{bmatrix} + C \frac{d}{dt} \begin{bmatrix} v_{c\_d} \\ v_{c\_q} \end{bmatrix} + C\omega \begin{bmatrix} -v_{c\_q} \\ v_{c\_d} \end{bmatrix} \quad - 4$$

where *Rg* represents the resistance in inductor *Lg*, *Rinv* stands for the resistance in inductor *Linv*, and □ is the grid-frequency. Similar to the PR controller, the vector controller usually consists of an outer-loop controller plus an inner-loop current controller as shown in Fig. 5. To develop the inner current controller for an LCL inverter, the conventional strategy is usually to omit the capacitor impact. Hence, (2) to (4) are simplified as (5), in which items *v'd* and *v'q* in brackets are used to design PI controllers for the *d*- and *q*-axis loops, and the other terms are treated as compensation items. This approximation would cause a decoupling inaccuracy and instability of the controller. In Fig. 5, *Leq=Linv+Lg*, *i*g_d* and *i*g_q* represent reference *d*- and *q*-axis currents at the PCC, and □ is assumed to be given through a phase-locked loop (PLL) method.

$$v_{inv\_d} = \underbrace{\left(R_{inv} + R_g\right) i_{g\_d} + \left(L_{inv} + L_g\right) \frac{di_{g\_d}}{dt}}_{v'_d} - \omega\left(L_{inv} + L_g\right) i_{g\_q} + v_{g\_d} \quad 5a$$

$$v_{inv\_q} = \underbrace{\left(R_{inv} + R_g\right) i_{g\_q} + \left(L_{inv} + L_g\right) \frac{di_{g\_q}}{dt}}_{v'_q} + \omega\left(L_{inv} + L_g\right) i_{g\_d} + v_{g\_q} \quad 5b$$

By forcing the PCC *q*-axis voltage equal to zero and aligning the *d*-axis voltage along with the grid PCC voltage which can be implemented through a PLL action, the instant active and reactive powers transferred from the inverter to the AC system are proportional to grid PCC *d*- and *q*-axis currents, respectively, as shown by:

$$p(t) = \left(v_{g\_d} \cdot i_{g\_d} + v_{g\_q} \cdot i_{g\_q}\right)/2 = v_{g\_d} \cdot i_{g\_d}/2 \quad (6a)$$

$$q(t) = \left(v_{g\_q} \cdot i_{g\_d} - v_{g\_d} \cdot i_{g\_q}\right)/2 = -v_{g\_d} \cdot i_{g\_q}/2 \quad (6b)$$

C) ARTIFICIAL NEURAL NETWORKS

Artificial neural networks are computational models inspired by the human brain, which can acquire and retain knowledge. Among the various neural network architectures, there is the architecture of multiple layers, called MLP (Multilayer Perceptron). This type of architecture is usually used for pattern recognition, functional approximation, and identification. The structure of a neural network can be developed according to Fig. 3.

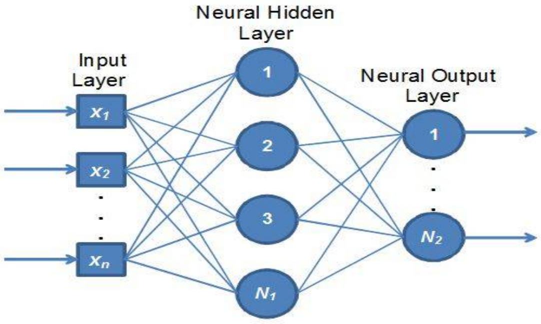

Fig. 2 Artificial Neural Network

As seen in Fig. 3, the neural network structure is basically composed of an input layer, hidden neural layers and an output neural layer. Also, between the layers, there is a set of weights, which are represented by a matrix of synaptic weights that will be adjusted during the training phase. It is further worth commenting that, for each of the neurons (hidden neural layers and output neural layer), it is necessary to implement activation functions in order to limit their output.

D) INCREMENTAL CONDUCTANCE MPPT

In incremental conductance method the array terminal voltage is always adjusted according to the MPP voltage it is based on the incremental and instantaneous conductance of the PV module.

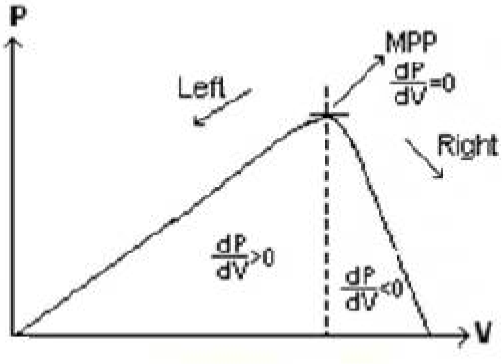

Fig-3: Basic idea of incremental conductance method on a P-V Curve of solar module

Fig-6 shows that the slope of the P-V array power curve is zero at The MPP, increasing on the left of the MPP and decreasing on the Right hand side of the MPP. The basic equations of this method are as follows.
$dI\ dV = -I\ V$ At MPP (3)
$dI\ dV > -I\ V$ Left of MPP (4)
$dI\ dV < -I\ V$ Right of MPP (5)
Where I and V are P-V array output current and voltage respectively. The left hand side of equations represents incremental conductance of P-V module and the right hand side represents the instantaneous conductance. When the ratio of change in output conductance is equal to the negative output conductance, the solar array will operate at the maximum power point.

IC MPPT ALGORITHM

This method exploits the assumption of the ratio of change in output conductance is equal to the negative output Conductance Instantaneous conductance. We have,

$$P = V I \quad (6)$$

Applying the chain rule for the derivative of products yields to

$$\partial P/\partial V = [\partial(VI)]/\partial V \quad (7)$$

At MPP, as $\partial P/\partial V=0$ (8)

The above equation could be written in terms of array voltage V and array current I as

$$\partial I/\partial V = -I/V \quad (9)$$

The MPPT regulates the PWM control signal of the dc – to – dc boost converter until the condition: $(\partial I/\partial V) + (I/V) = 0$ is satisfied. In this method the peak power of the module lies at above 98% of its incremental conductance. The Flow chart of incremental conductance MPPT is shown below.

E) INTEGRATING MPPT AND ANN CONTROLS

The main considerations for integration of MPPT and ANN controls include:
1) How the integration may affect MPPT efficiency and speed,
2) How to maintain the stability of DC link voltage under variable output power of a PV array
3) How to provide reliable reactive power or grid voltage regulations at the PCC in the integrated condition.
Fig. 7 shows the overall system structure.

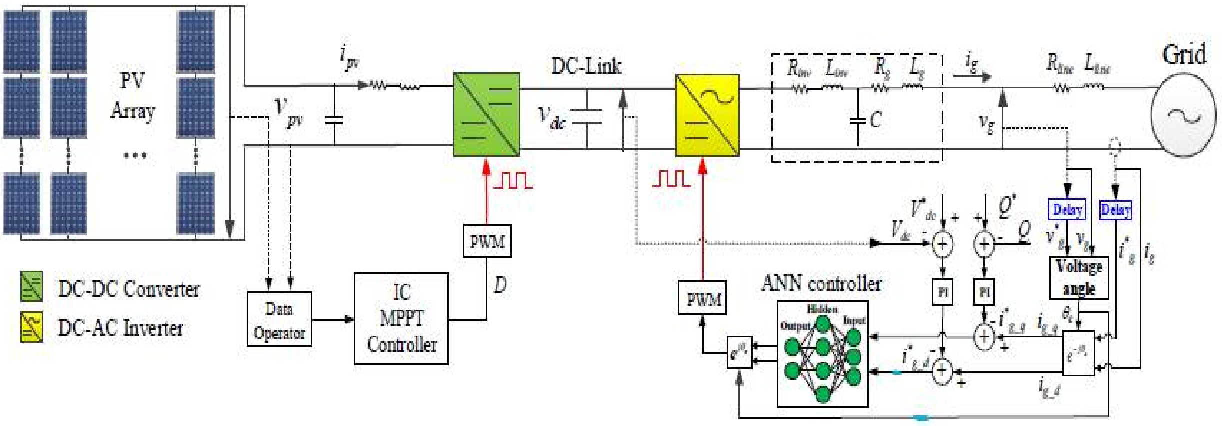

Fig. 4. Neural network for MPPT and grid integration of residential solar PV system

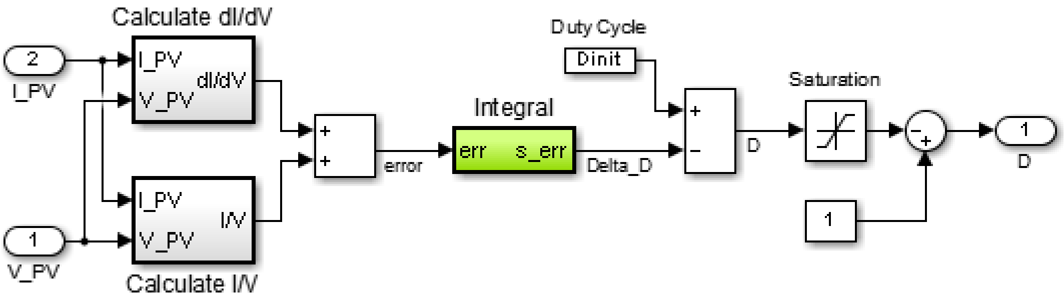

Fig 5 MPPT Control for DC-DC converter

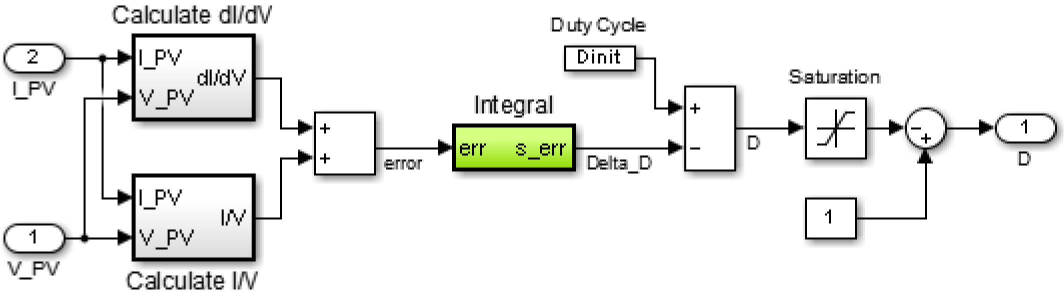

Fig 6 ANN Control for DC-AC inverter

A. Maximum Power Extraction Control

This paper uses the IC MPPT approach to extract the maximum power from a PV array. The IC MPPT controller was initially tuned by considering the PV array and DC-DC converter only under a constant DC-link voltage condition.

After the MPPT controller is tuned, the PV array is connected to the grid through the single-phase inverter. However, the integration may cause large oscillation of the DC-link voltage, especially under intermittent solar irradiance conditions. This may affect the MPPT efficiency and potential trip of the PV MPPT Control for DC-DC converter ANN Control for DC-AC inverter system. Thus, maintaining the stability of DC-link voltage is critical for connecting the PV system to the grid.

B. Artificial Neural Network Control

An ADP-ANN controller must be trained before applying it to the overall PV system. The ANN was trained repeatedly to track a variety of reference d-q current trajectories until satisfactory and excellent tracking performance is achieved. Each training experiment starts with randomly generated network weights. Thus, each may converge to different ADP cost. The final network weights are selected from those training experiments having the lowest ADP costs. After the network is well trained, the ANN controller for simulation or experiment case is able to track reference *d-q* current with minimum errors and in the optimal way according to ADP.

C. Integrating MPPT and ANN Controls

The integration of MPPT and ANN controllers is based on the PV system shown by Fig. 7. The MPPT controller is responsible for extracting power from the PV array with the maximum efficiency. Depending on the irradiance levels, the extracted power could go up and down, causing the DC-link voltage to increase and decrease. The stability of the DC-link voltage is maintained through the ANN controller. To achieve this, a PI-based DC-link voltage controller is added before the ANN current tracking controller. According to 6(a), this is achieved through the control of the PCC d-axis current. As shown by Fig. 7, the DC-link voltage controller generates a d-axis current reference to the ANN controller based on the error signal between the measured and reference DC-link voltages.

The q-axis current tracking ability of the ANN controller is used for another control purpose. According to 6(b), this could be either reactive power control or grid voltage support control at the PCC. For reactive power control, a PI-based reactive power controller is added before the ANN current tracking controller. The reactive power controller generates a q-axis current reference to the ANN controller based on the error signal between the measured and reference PCC reactive power. For grid voltage support control at the PCC, a PI-based PCC voltage controller is used to generate a *q*-axis current reference to the ANN controller based on the error signal between the measured and reference PCC voltages. Certainly, the controller gains of the PCC voltage controller would be different from those of the reactive power controller.

The PI gains of the DC-link voltage controller and reactive power or PCC voltage support controller were initially tuned without considering the PV array and MPPT control. Also, the ANN controllers are trained for current tracking purpose only. Thus, detailed performance evaluation of the overall integrated system is needed and important. This is discussed in Sections VI and VII, in which we found that PI gains of the DC-link voltage controller and the reactive power or PCC voltage controller usually need to be re-tuned through trial and error to achieve the best control performance regarding the stability and response speed, particularly if the ANN current controller is replaced by a conventional current controller.

The Simulink implementation of the MPPT and ANN control algorithms is also shown in Fig. 7. Within the MPPT algorithm, dI_{pv}/dV_{pv} and I_{pv}/V_{pv} are first calculated based on PV array terminal voltage and current. Then, the summation of $dI_{pv}/dV_{pv} + I_{pv}/V_{pv}$ is used to determine ΔD, the duty cycle correction, to update duty ratio for control of the DC-DC converter. Within the ANN control algorithm, the PCC voltage Vg is used to determine the angular position of Vg, which is needed for transformation of the PCC sinusoidal current to its *dq* representation and inverse transformation of *dq* control voltage to its sinusoidal representation. The outer loop controller produces the reference *dq* current based on DC -link voltage and PCC reactive power. The difference between the measured and reference *dq* currents is used to produce the error and integral of error terms for the ANN controller. The *dq* control voltage generated by the ANN is converted into sinusoidal voltage for control of the DC-AC inverter.

IV. SIMULATION RESULTS

The proposed work is completed on MATLAB software on the version of R2014a. The designed circuits were drawn and simulated using MATLAB Simulink and Sim power system toolboxes.

The proposed system, to simulate an artificial neural network (ANN) control strategy based on approximate dynamic programming (ADP) for optimal control and grid integration of residential solar PV systems.

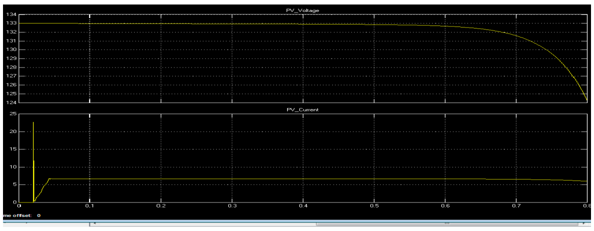

Fig 7 PV output

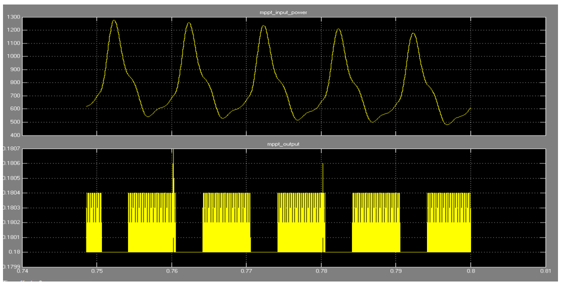

Fig 8 MPPT input & output

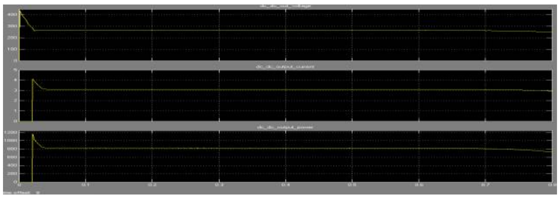

Fig 9 Boost converter input

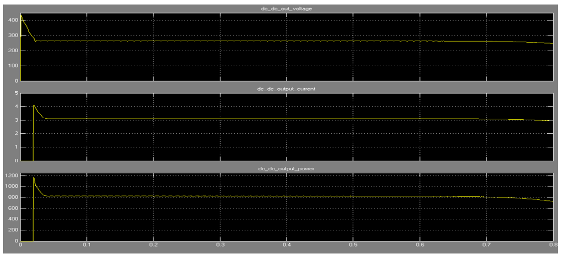

Fig 10 Boost converter output

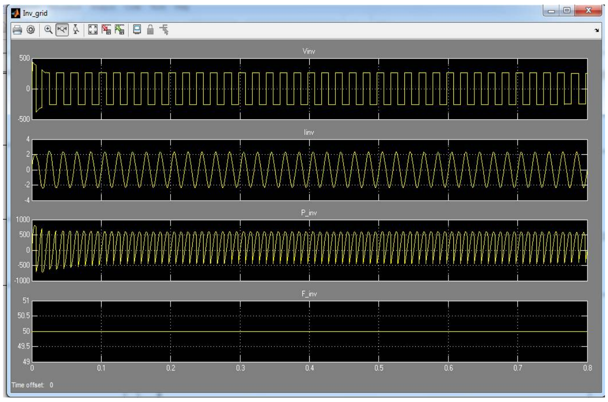

Fig 11 Inverter output

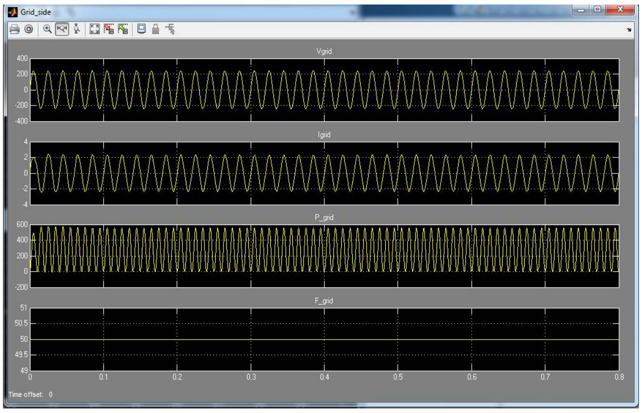

Fig 12 Grid output

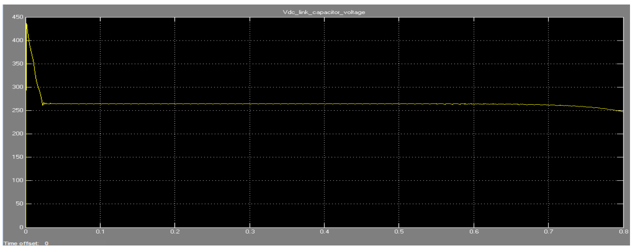

Fig13 DC link capacitor voltage

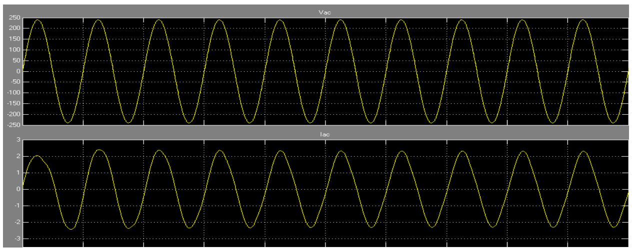

Fig 14 AC Load output

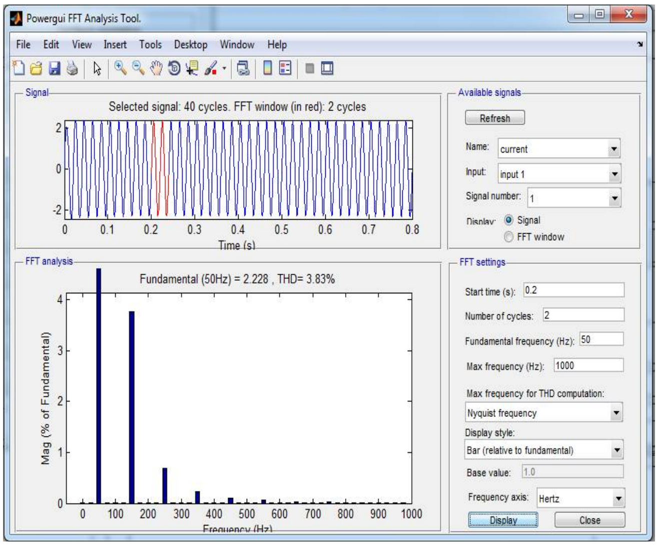

Name: current
Input: input 1
Signal number: 1
Display: ● Signal ○ FFT window
Start time (s): 0.2
Number of cycles: 2
Fundamental frequency (Hz): 50
Max frequency (Hz): 1000
Max frequency for THD computation: Nyquist frequency
Display style: Bar (relative to fundamental)
Base value: 1.0
Frequency axis: Hertz

Fig 13 Threshold value

V. CONCLUSION

This project proposes a single-phase, river top solar PV system based on artificial neural networks for control and grid integration of a solar photovoltaic array through an LCL-filter based inverter. The proposed artificial neural network controller implements the optimal control based on the approximate dynamic programming. The simulation results demonstrate that the solar PV system using the ADP-based artificial neural network controller has more improved performance than that using the proportional resonant or conventional standard vector control techniques, such as no requirement for damping resistance, more reliable and efficient extraction of solar power, more stable DC-link voltage, and more reliable integration with the utility grid. Using the ADP-based neural network control technique, the harmonics are significantly reduced and the system shows much stronger adaptive ability under uncertain conditions, which would greatly benefit the integration of small-scale residential solar photovoltaic systems into the grid.

REFERENCES

[1] Renewable Energy World Editors. (2014, Nov. 12). Residential Solar Energy Storage Market Could Approach 1 GW by 2018. Available: http://www.renewableenergyworld.com.
[2] R. A. Mastromauro, M. Liserre and A. D. Aquila, “Control Issues in Single-Stage Photovoltaic Systems: MPPT, Current and Voltage Control”, *IEEE Trans. Ind. Informatics,* vol. 8, no. 2, pp. 241-254, May 2012.
[3] E. Lorenzo, G. Araujo, A. Cuevas, M. Egido, J. Miñano and R. Zilles, *Solar Electricity: Engineering of Photovoltaic Systems*, Progensa, Sevilla, Spain, 1994.
[4] J. M. Carrasco, L. G. Franquelo, J. T. Bialasiewicz, E. Galván, R. C. P. Guisado, M. Á. M. Prats, J. I. León, and N. Moreno-Alfonso, “Power-Electronic Systems for the Grid Integration of Renewable Energy Sources: A Survey”, *IEEE Trans. Ind. Electron.*, vol. 53, no. 4, pp. 1002-1016, August 2006.
[5] W. T. Franke, C. Kürtz and F. W. Fuchs, "Analysis of control strategies for a 3 phase 4 wire topology for transformer less solar inverters," in *Proc. IEEE Int. Symp. Ind. Electron.*, Bari, pp. 658-663, 2010.
[6] B. Karanayil, V.G. Agelidis, and J. Pou, "Performance Evaluation of Three-Phase Grid-Connected Photovoltaic Inverters Using Electrolytic or Polypropylene Film Capacitors," *IEEE Trans. Sustain. Energy*, vol. 5, no. 4, pp. 1297-1306, Oct. 2014.
[7] B. Bahrani, A. Rufer, S. Kenzelmann, and L. A. C. Lopes, “Vector control of single-phase voltage-source converters based on fictive-axis emulation,” *IEEE Trans. Ind. Appl.*, vol. 47, no. 2, pp. 831–840, Mar./Apr. 2011.
[8] M. Castilla, J. Miret, J. Matas, L. G. Vicuña, and J. M. Guerrero, "Linear Current Control Scheme With Series Resonant Harmonic Compensator for Single-Phase Grid-Connected Photovoltaic Inverters," *IEEE Trans. Ind. Electron*., vol. 55, no. 7, pp. 2724–2733, July 2008.
[9] A. Abrishamifar, A.A. Ahmad, and M. Mohamadian, "Fixed Switching Frequency Sliding Mode Control for Single-Phase Unipolar Inverters," *IEEE Trans. Power. Electron*., vol. 27, no. 5, pp. 2507–2514, May 2012.
[10] M. El-Habrouk, M.K. Darwish, and P. Mehta, "Active power filters: A review," *IEEE Proc. Electric Power Applicat.*, vol.147, no 5, pp. 403–413, Oct. 2000.
[11] J. Lettl, J. Bauer, and L. Linhart, "Comparison of different filter types for grid connected inverter," in *Proc. Progress in Electromagnetics Research Symp.*, Marrakesh, Morocco, 2011, pp. 1426-1429.

[12] J. Dannehl, C. Wessels, and F. W. Fuchs, “Limitations of voltage oriented PI current control of grid-connected PWM rectifiers with LCL filters,” *IEEE Trans. Ind. Electron*., vol. 56, no. 2, pp. 380–388, Feb. 2009.

[13] Z. Xin, P. C. Loh, X. Wang, F. Blaabjerg and Y. Tang, "Highly Accurate Derivatives for LCL-Filtered Grid Converter with Capacitor Voltage Active Damping,” *IEEE Trans. Power. Electron*., vol. 31, no. 5, pp. 3612-3625, May 2016.

[14] H. Arritt, "Protection Practices fr an Integrated Grid," in *Proc. IEEE Power & Energy Soc. General Meeting*, Denver CO, USA, 2015.

[15] M. Veerachary, T. Senjyu and K. Uezato, "Neural-network-based maximum-power-point tracking of coupled-inductor interleaved-boost converter- supplied PV system using fuzzy controller," *IEEE Trans. Ind. Electron*., vol. 50, no. 4, pp. 749-758, Aug. 2003.